Elemental and neurochemical based analysis of the pathophysiological mechanisms of Gilles de la Tourette syndrome

Ahmad Seif Kanaan

Max Planck Institute for Human Cognitive and Brain Science, Leipzig, Germany
* kanaan@cbs.mpg.de.

Abstract: Brief statement of work in English (max**. 80 words).**

Zusammenfassung: Kurze Zusammenfassung der Arbeit auf Deutsch, max. 80 Wörter.

Introduction

Gilles de la Tourette syndrome is a neuropsychiatric movement disorder characterized by tics and the presence of associated comorbid conditions. Although a range of treatments are currently being used to manage the symptomatology of GTS, there is currently no cure for the manifesting motor and non-motor features. This is largely due to the lack of a comprehensive pathophysiological model, which may be attributable to the dearth of studies utilizing multi-parametric imaging approaches. As such, there is an urgent need in further elucidating the nature of GTS pathophysiology to accelerate the drug discovery and development process.

At the neurochemical level, abnormalities in dopaminergic neurotransmission are widely considered as a primary abnor- mality in GTS [1]. However, in view of the strict spatio-temporal synergy exhibited between excitatory, inhibitory and modulatory neurochemical systems that drive typical motor and non-motor behaviour, several groups have posited that other neurochemical systems may exhibit perturbations as well [1]. Along this line, recent studies have implicated other systems that most prominently include the γ-Aminobutyric acid (GABA)-ergic system [1]. Although GABA exhibits both spatio-temporal as well close metabolic links to glutamate (Glu), investigations on the role of the glutamatergic system in GTS have not yet been undertaken in vivo. At the elemental level, one unifying feature exhibited by excitatory, inhibitory and modulatory neurotransmitter systems is that the enzymes involved in their metabolism and the production of their receptors/transporters, require the element iron for typical function. Along this line, preliminary work investigating serum ferritin concentrations have indicated that iron may be related to GTS pathophysiology. Nevertheless, in vivo investigations of the role of brain iron in GTS pathophysiology are currently lacking.

With recent advances in quantitative Magnetic Resonance (MR) techniques, a unique perspective that allows the in vivo measurement of biochemical and physio-chemical tissue properties has been afforded, thus paving the road for undertaking more incisive investigations of disease specific changes at multiple-scales in vivo. Proton Magnetic Resonance Spectroscopy (^{1}H-MRS) and Quantitative Susceptibility Mapping (QSM) are two such approaches that allow the measurement of steady-state metabolite quantities and the intrinsic physical property of magnetism in matter. Using ^{1}H-MRS, for example, several neurochemicals could be quantified, including surrogate measures related to glutamatergic signalling. On the other hand, QSM is a novel contrast mechanism that provides surrogate quantitative measures of biomarkers such as iron.

Strategy

Utilizing a multi-parametric, quantitative MRI approach in vivo, we investigated the role of Glu and iron in GTS using ^{1}H-MRS and QSM, respectively. To achieve these aims, two methodological investigations were initially conducted to obtain quantitative neurochemical and susceptibility measurements of sufficient precision to identify rather subtle changes. MR and clinical data were acquired from a well-characterized sample of adult patients with GTS (N=40) and age/gender matched healthy controls (N=40). MR measurements were performed on a 3T MAGNETOM Verio (Siemens Healthcare, Erlangen, Germany) with a 32-channel head coil. T1-weighted data were acquired using an MP2RAGE sequence (TR=5s; TE=3.93ms; TI=0.7/2.5s; 256x256 matrix; 1.0mm^3 isotropic). Proton spectra were acquired using PRESS from the striatum, thalamus and the cingulate cortex (TE= 30ms, TR=3s, 1024 data points; FASTESTMAP shimming, 6 unsuppressed, 80/128

suppressed). To interrogate the influence of treatment on neurochemical and clinical characteristics of the study sample, we employed a longitudinal study design in which the patients were invited to undergo treatment with the commonly used antipsychotic aripiprazole. Susceptibility-weighted data were acquired using FLASH with TR=30ms; TE=17ms; 256x256 matrix; flip-angle=13; 0.8mm^3 resolution. A 10ml blood sample was also collected for the quantitation of serum ferritin. To investigate associations between magnetic susceptibility differences and default transcriptional levels of iron-related genes, microarray gene-expression data were extracted from the Allen Human Brain Atlas, which provides 20,737 annotated gene-expression profiles from 3702 tissue samples specific MNI coordinates across the whole brain from 6 post-mortem samples [2].

Pathological glutamatergic neurotrans-mission in Gilles de la Tourette syndrome

To ensure the reproducibility of our neurochemical measurements, we first examined the test-retest reliability of absolute metabolite quantitation with the consideration of the variabilities of within voxel tissue proportions across subjects and sessions [3]. We observed that sophisticated and commonly used segmentation algorithms yield different regional estimates of within voxel tissue fractions in a sample of healthy controls scanned twice (N=23) [3]. One tissue segmentation algorithm (SPM) yielded a high consistency in the estimation of between session tissue proportions relative to others. Considering the algorithm's estimates of within voxel tissue proportions for the correction of absolute metabolite quantities, we observed a decrease in the variance of absolute estimates of key metabolites that include Glu and glutamine (Gln).

This methodological investigation led to the conclusion that the careful consideration and utility of reliable segmentation algorithms is essential for the interrogation of changes in relevant metabolite concentrations in psychiatric and neurological disorders, thus better informing our examination of the role of Glu in GTS pathophysiology.

Given the difficulty of acquiring high quality spectra in subcortical regions, especially in a patient population characterized by movement, we employed a careful acquisition and processing scheme that incorporated (a) an automated voxel re-localization technique [4]; (b) the removal of motion corrupted outlier signals; (c) frequency- and phase-drift correction in the time domain [5]; (d) absolute metabolite quantitation with the consideration of within voxel compartmentation; and (e) a semi-automated quality assessment protocol [6] (Fig. 1). By utilizing these techniques, we observed a high reliability of voxel re-localization and metabolite quantitation across sessions in the healthy control sample [3].

Figure 1: Spectral data preprocessing. (A) As MRS measurements involve the summation of multiple averages to build the SNR, subject motion and drifts in the magnetic

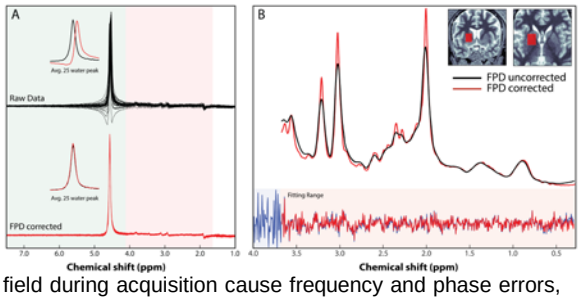

field during acquisition cause frequency and phase errors, which may give rise to incoherent signal averaging, line broadening, line shape distortion and reduced signal-to-noise ratio, which may ultimately affect metabolite quantitation and group comparisons. As such, non-averaged time- domain raw data were exported from the scanner and a non-linear least-squares minimization operation was used to fit each signal average to a reference scan by the adjustment of the frequency and phase of the signal [5]. The effect of frequency- and phase-drift (FPD) correction on data acquired from a striatal voxel of a GTS patient (top) is clearly visible in the corrected data (bottom). The performance of the non-linear minimization operation is illustrated on a single scan (the 25th average) superimposed on the reference signal (inset plots). For the aMCC spectra, which exhibited a high signal-to-noise ratio (SNR), spectral registration was conducted on an approximate range between 1.8–4.2 ppm (red shaded area). For spectra with a lower SNR, the strength of the water signal was used for spectral registration on an approximate range between 4.2–7.5 ppm (green shaded area). (B) The benefit of the correction on the linewidth and SNR is clearly visible on the red coloured spectrum. As some of the spectra exhibited a spurious residual signal in the ppm range between 3.6–4.0 ppm (blue shaded area), possibly due to insufficient spoiling, the LCModel fitting range was adjusted to 0.2–3.67 ppm (orange shaded area).

Comparing the healthy control group with the GTS sample at baseline, we observed significant reductions in striatal concentrations of Gln, Glu + Gln (Glx) and the Gln:Glu ratio, and thalamic concentrations of Glx in GTS (Fig. 2). ON-treatment patients exhibited no significant metabolite differences when compared to controls but significant increases in striatal Glu and Glx, and trends for increases in striatal Gln and thalamic Glx compared to baseline measurements. Multiple regression analysis revealed a significant negative correlation between (a) striatal Gln and actual tic severity; and (b) thalamic Glu and premonitory urges (Fig. 2).

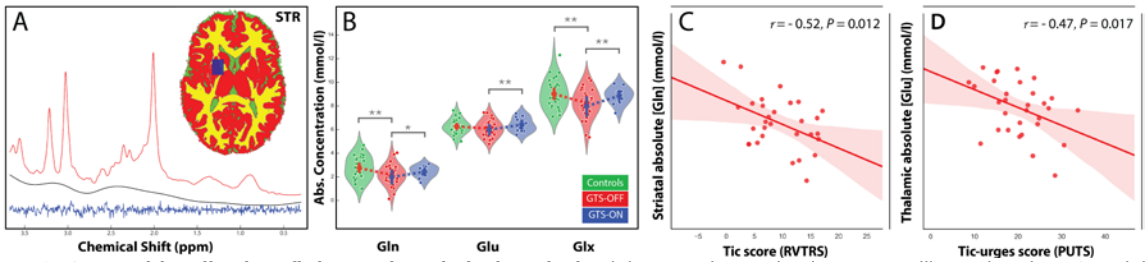

Figure 2: Spectral localization, fitting and statistical analysis. (A) Exemplary striatal spectrum illustrating the LCModel fit, baseline and residual signals of frequency- and phase-drift-corrected data. The inset images demonstrate the location of the region of interest with respect to the grey matter, white matter and CSF compartments, which were used to calculate within-voxel tissue proportions for absolute quantitation correction. (B) Violin plots illustrating the distribution of Gln, Glu and Glx concentrations in controls (green), GTS patients at baseline (red) and GTS patients following treatment with aripiprazole (blue); **P < 0.05; *denotes a trend for significance (P < 0.1). (C,D) Correlation of absolute metabolite concentrations with clinical measures using a multiple linear regression model revealed significant negative correlations between (C) left corpus striatal Gln concentrations and post-scan measurements of actual tic severity (modified RVTRS), in addition to (D) bi-lateral thalamic Glu concentrations and pre-monitory urges (PUTS).

Given the interdependent metabolic relationship exhibited between Glu and GABA via the non-neuroactive intermediate Gln, our results indicate that patients with GTS exhibit an abnormality in the flux of metabolites in the GABA-Glu-Gln cycle (Fig. 3). In general, this implies the presence of perturbations in subcortical astrocytic-neuronal metabolic coupling (ANMC) systems that maintain the subtle balance between excitatory and inhibitory neurotransmission as reported via gene-set analyses [7]. Such perturbations may ultimately lead to spatially focalized alterations in neurochemical ratios in functionally distinct striatal subdivisions, which would have a profound influence on the mechanisms involved in reinforcement learning and habit formation systems that are governed by striatal neurons that code the serial order of syntactic natural behaviour.

Subcortical Iron reductions associated with neurochemical abnormalities in GTS

In our next line of questioning, we focused on the element iron in view of the crucial role it exhibits in varied biochemical mechanisms sustaining developmental processes and neurochemical pathways. Based on the results achieved in the 1H-MRS study and preliminary work indicating reductions in the iron sequestering protein ferritin in both children and adults, we postulated that patients with GTS exhibit abnormalities in iron metabolism, which may influence mechanisms of subcortical neurotransmission. We employed QSM to estimate subcortical susceptibility values and relating these to (a) gene-expression levels of iron-related genes extracted from the Allen Human Brain Atlas (AHBA) and (b) 1H-MRS measures of Glu signalling markers.

In general, QSM images are reconstructed from tissue phase maps that are typically generated by combining signals recorded by multi-channel coil elements. However, the coil-combination of multi-channel data is often degraded and may contain pole artifacts as exhibited by the widely used Adaptive Combine (AC) technique. Comparing subcortical susceptibility values obtained following coil-combination with the AC technique and a novel method (EPIRiT-SVD) that does not produce pole artifacts [9], significant susceptibility differences in regions implicated in GTS pathophyiology (e.g. Striatum, Thalamus) were observed. This methodological investigation indicated that pole artifacts significantly corrupt QSM data and may bias inter-group comparisons.

Utilizing the ESPIRiT-SVD coil combination algorithm, we achieved tissue phase maps without any pole artifacts for QSM reconstruction (super-fast dipole inversion [10]) in the control and GTS samples (Fig 4.). We focused on estimating magnetic susceptibility in subcortical nuclei implicated in GTS pathophysiology and also exhibit high concentrations of iron and the neurotransmitters dopamine, Glu and GABA. Our results indicated that GTS patients exhibit significant reductions of magnetic susceptibility in basal ganglia, brain-stem and cerebellar nuclei (Fig. 4), and were mirrored by decreases in serum ferritin levels (Fig. 5A). Serum ferritin levels were positively correlated with susceptibility values in basal ganglia and brainstem nuclei in the entire sample (Fig. 5B). By employing Principal Component Analysis (PCA) to reduce the clinical data into a set of clinical scores, we observed that both striatal magnetic susceptibiliy and serum ferritin levels were negatively correlated with the principal component representing a composite motor-tic score (Fig. 5C-F).

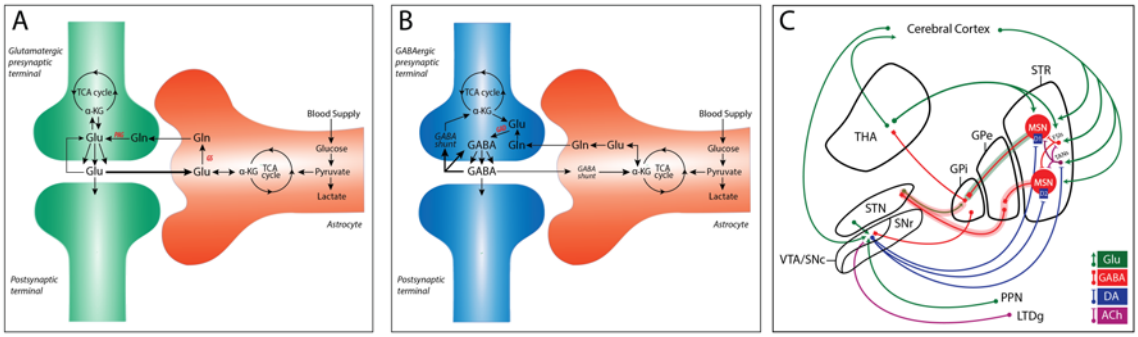

Figure 3: (A-B) Astrocytic-neuronal coupling and the homeostasis of glutamatergic and GABAergic neurotransmission. Glu and GABA exhibit close metabolic links, where GABA is directly synthesized from Glu via glutamate decarboxylase and is catabolized into Glu via transamination [8]. Given that neurons lack the enzyme pyruvate dehydrogenase, which is needed to link glycolytic metabolism to the TCA cycle, they are unable to replenish their vesicular concentrations of synaptically released Glu. As such, Gln plays an instrumental role in maintaining the homeostasis of Glu and GABA. The homeostatic mechanisms involved in the synthesis, degradation, and trafficking of Glu and GABA are instrumental in the maintenance of the subtle balance of excitation and inhibition. The observed decreases in striatal concentrations of Gln, Glx and the Gln:Glu ratio are consistent with the assumption that patients with GTS exhibit a dysfunctional astrocytic-neuronal coupling system (de Leuw,2015). **(C) Local circuit model of subcortical connectivity.** The basal ganglia operate through inhibition, dis-inhibition and facilitation, where the intrinsic quiescence of striatal neurons permits the output nuclei (GPi/SNr) to hold the thalamus under GABA-mediated tonic inhibition to prevent inappropriate movements. Select movements are facilitated upon the activation of striatal medium-sized spiny neuron populations that reduce the tonic pallido-thalamic output. Coordinated behaviour is thought to ensue as a result of the integrated output of the D1- (direct-pathway, shaded green) and D2- (indirect-pathway, shaded red) receptor mediated medium-sized spiny neurons, whose outputs arbitrate the selection of the ultimate program. Chronic perturbations in the flux of metabolites in the GABA-Glu-Gln cycle, could lead to spatially focalized alterations in excitatory and inhibitory neurotransmitter ratios and subsequent abnormalities in the archetypical dynamics of tonic/phasic dopamine signalling. Such perturbations may have a profound influence on the neuro-plastic mechanisms involved in reinforcement learning and habit formation systems.

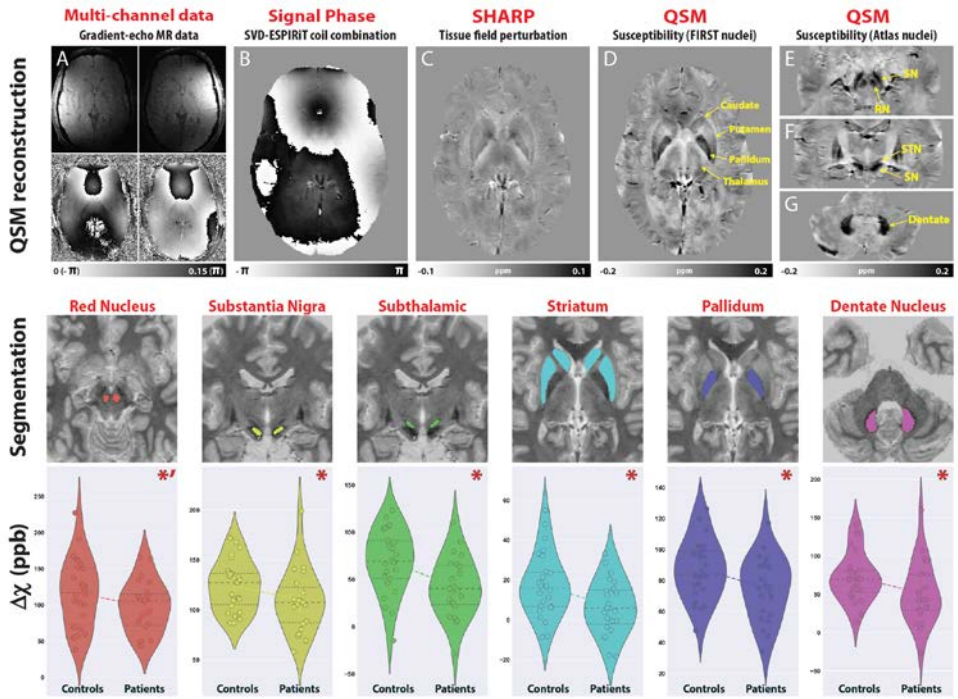

Figure 4: Quantitative Susceptibility Mapping in Gilles de la Tourette syndrome. Upper panel: Quantitative Susceptibility Mapping. Representative images from one GTS patient illustrating the quality of the (A) raw magnitude and phase single-channel data, and (B) signal phase following multi-channel coil combination with the SVD-ESPIRiT method (SI text). Magnetic susceptibility maps were estimated using the superfast dipole inversion approach, which utilizes Sophisticated Harmonic Artifact Reduction for Phase (SHARP) to eliminate background field contributions (C), and threshold k-space division (TKD) for solving the ill-posed inverse problem from tissue field perturbation to magnetic susceptibility. The sharp deposition of iron is clearly visible in (D) basal ganglia nuclei, whose masks were generated automatically using the FSL-FIRST segmentation algorithm performed on a QSM-MP2RAGE hybrid contrast images; and (E,F,G) brainstem/cerebellar nuclei, whose masks were generated by non-linear transformation of atlas-based masks that were carefully delineated on a QSM group average template in MNI space. Lowerpanel: Nucleus segmentation quality and group comparison statistics. GTS patients exhibited significant susceptibility reductions, passing FDR multiple comparison correction in the red nucleus (RN), substantia nigra (SN), subthalamic nucleus (STN) and striatum. These effects were mainly driven by reductions in left hemisphere nuclei as illustrated by the split violin plots. (* denotes significance at P FDR ¡0.05 and *' denotes trends for significance at P FDR <0.1)

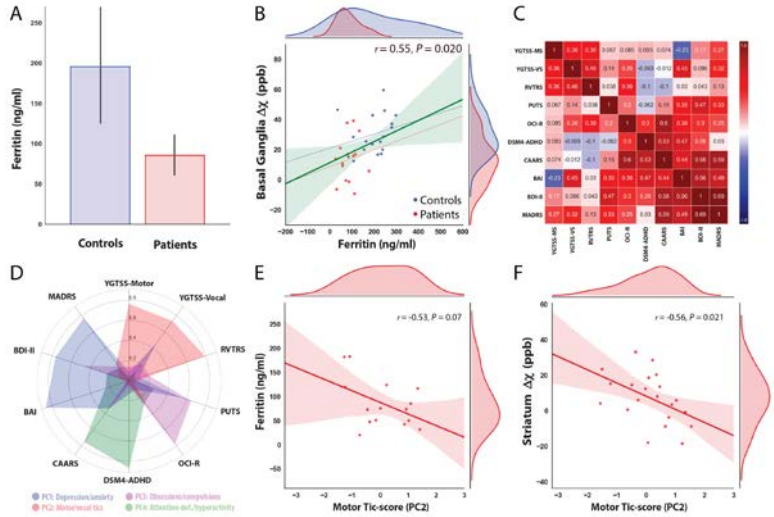

Figure 5: Examination of serum ferritin differences and their relationship to magnetic susceptibility and clinical scores. (A) Reductions in serum ferritin levels were observed in GTS compared to the healthy controls. (B) Serum ferritin exhibited a significant positive correlation with magnetic suscep- tibility in the entire sample. (C) The correlation matrix between all the acquired clinical variables revealed sufficient complementary for data-reduction using PCA. (D) Four principal components explaining 79% of the variance were extracted using PCA. These represented scores for (i) depression/anxiety, (ii) motor-tics, (iii) obsessions/compulsions and (iv) attention-deficit/hyperactive behaviour. The principal component representing a composite motor-tic score exhibited negative correlations with (E) serum ferritin and (F) striatal magnetic susceptibility.

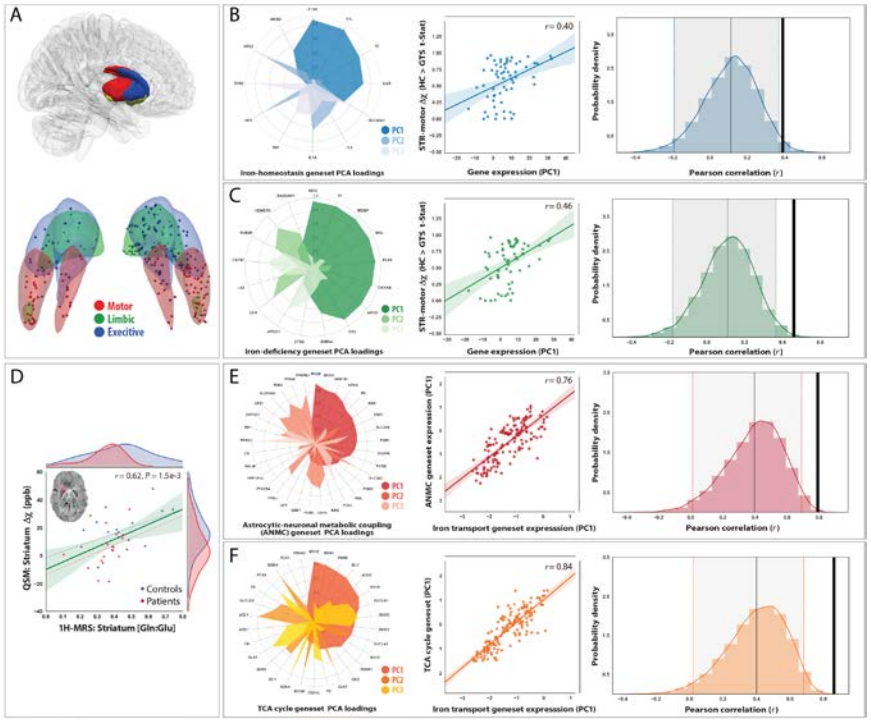

Figure 6: **(A,B,C) Examining the relationship between magnetic susceptibility and iron-related gene expression**. (A) Illustration of the location of tissue samples extracted for gene-expression analysis by the AHBA in distinct striatal regions (MNI coordinate space). The principal component scores of genesets representing iron-homeostasis (B) and iron-deficiency (C) exhibited significant correlations with statistical maps representing magnetic suscepti- bility reductions in the motor striatum (fsl-randomise, 10,000 permutations, TFCE). **(D,E,F) Examining the relationship between surrogate measures of iron and neurochemical signalling.** (D) A multiple-linear regression model accounting for age, gender and image quality revealed a significant positive correlation between striatal susceptibility levels and ^{1}H-MRS measures of the Gln:Glu ratio. A similar effect was also observed at the genetic level, as we demonstrate that the principal component scores of iron-transport genes exhibit correlations with genesets describing (E) astrocytic-neuronal metabolic coupling (ANMC) and the (F) TCA cycle. Principal component loadings for all genes sets are illustrated in the polar plot of the (B,C,E,F, left-panels). To statistically evaluate whether the observed correlations (mid-panel) were higher than what would be expected under the null-condition, a permutation based approach was implemented (B,C,E,F, mid-panels). A null distribution was constructed using a resampling based approach with 10,000 permutations with random sampling of genes from 20,373 annotated genes from AHBA. The null hypothesis was rejected if the observed correlation exceeded an alpha level of 0.05. All correlations exhibited significance (B,C,E,F right-panels). All genesets were retrieved from the Molecular Signature Database.

Moreover, we examined the role of iron-related genes extracted from AHBA on magnetic susceptibility differences between patients and controls. We observed that default transcriptional levels of iron-related gene-sets (iron-homeostasis, iron deficiency, iron-transport, ferritin genes) extracted from the motor striatum are positively correlated to statistical maps of magnetic susceptibility reductions in the same MNI coordinates (Fig 6A).

To interrogate possible relationships between iron and neurochemical abnormalities in GTS, we observed a relationship between striatal susceptibility levels and 1H-MRS concentrations of the Gln:Glu ratio (Fig. 6D). This relationship was also observed at the genetic level, as we demonstrate that expression levels of the iron-transport geneset exhibit significant positive correlations with the astrocyte-metabolic coupling (ANMC) geneset; which has been previously implicated in GTS [7] and is involved in metabolic processes related to GABA-Glu-Gln cycling (Fig. 6E). The iron-transport geneset was also strongly correlated with a gene-set describing the TCA cycle (Fig. 6F). Put together, these results suggest that patients with GTS exhibit disturbances in iron regulatory systems in subcortical regions, which may have a strong influence on mechanisms sustaining GABA-Glu-Gln metabolism.

Conclusion

Our results indicate that patients with GTS exhibit an abnormality in the flux of metabolites in the GABA-Glu-Gln cycle, thus implying perturbations in astrocytic- neuronal coupling systems that maintain the subtle balance between excitatory and inhibitory neurotransmission within subcortical nuclei. These abnormalities may be driven or further compounded by abnormalities in iron metabolism. Chronic perturbations in the subcortical GABA-Glu-Gln cycle flux could lead to spatially focalized alterations in excitatory, inhibitory and modulatory subcortical neurochemical ratios that would have a profound influence on the neuroplastic mechanisms involved in reinforcement learning and habit formation systems. This work sheds a new light on the neurobiological basis of GTS and provides novel clues that may prove critical in the future development of functionally selective pharmacological modulators that target multiple neurochemical systems.

References

1. Singer, H. (2013). Tourette Syndrome (Oxford University Press), 276–297.

2. Hawrylycz MJ, et al. Nature 2012; 489: 391–399.

3. Kanaan, A., et.al (2015). Proc. Intl. Soc. Mag. Reson 23, 1974.

4. Dou, W., et al (2015). Magnetic Resonance Materials in Physics, Biology and Medicine, 259–270.

5. Near, J., et al (2015). Magnetic Resonance in Medicine. 73, 44–50.

6. Kanaan, A. S., et al. (2017). BRAIN 140, 218–234.

7. De Leeuw, C., et al (2015). European Journal of Human Genetics 23, 1–4 .

8. Waagepetersen, H.S., et al (2007).Handbook of neurochemistry and molecular neurobiology (SpringerS: New York) 1–21.

9. Metere, R., et al (2017). Proc. Intl. Soc. Mag. Reson 23, 2433.

10. Schweser, F., et al (2013). Magnetic Resonance in Medicine 69, 1582–1594 (2013).